

Reconstruction of Linear Folding Structures with the Use of Volume Balancing

F. L. Yakovlev

*Schmidt Institute of Physics of the Earth, Russian Academy of Sciences,
Bol'shaya Gruzinskaya ul. 10, Moscow, 123995 Russia*

Received May 15, 2009

Abstract—The structure of linear fold zones is considered as a set of objects of several hierarchic levels with specific kinematic models of their formation. The prefolded structure was reconstructed, and recent depths of the sedimentary cover base were predicted on the basis of these notions with the use of the Northwestern Caucasus folding as an example. Fold domains were used as the main objects. The basic parameters of their geometry (dips of axial surfaces, dips of fold system levels, shortening values) measured in natural structures were identified with the deformation ellipsoid. Three kinematic operations: rotation, simple horizontal shearing, and extension, which made it possible to reconstruct the horizontal layering and the position of the profile line segment for each domain. Eleven profiles were reconstructed by the consecutive joining of the prefolded states of the domains. The fold shortenings were obtained for these profiles and their 42 parts. The developed quasi-three-dimensional model of the natural structure demonstrates specific features important for the verification of geodynamic models.

PACS numbers: 91.55.Hj; 91.45.-c

DOI: 10.1134/S1069351309110111

INTRODUCTION

The problem of the formation of linear folding structures, which has existed for more than two centuries, has aspects that are both closely related to each other and independent. Of course, the construction of geodynamic models of such structures, which within the framework of plate tectonics are traditionally associated with convergent boundaries, is one of the most important aspects of this problem. In this investigation, particular attention is concentrated on the aspects of structural geology and mechanics. Linear folding structures are usually considered as a set of folds of several orders arising as a result of buckling. From the standpoint of structural geology, a complete linear folding is a complex object, because this structure cannot be exactly reconstructed (completed) to a large depth or into its eroded part. There are two possible limiting variants (see, for example, [Yaroshevskii, 1981]): (1) the use of regularities of “parallel” folding, which is restricted by the entire cover thickness and has a free space at the top and a common detachment at the bottom and (2) the completion of the structure on the basis of the laws of a “similar” folding, when the form of minor folds observed in the band of exposures spreads indefinitely upward and downward. The spectrum of intermediate variants is wide, and the choice of one of them or their combination usually depends on the theoretical position of the researcher. From the standpoint of mechanics, there are two models, which can be, in principle, used for the description of linear folding deformations: (1) the concept of the description of isometric structures in terms of the deformation ellipsoid for large defor-

mations and (2) the description of the stability loss and the stress states of layers for the variants of lateral buckling and transversal bending. The first model is used within the framework of strain analysis [Ramsay and Huber, 1987]; the second model is successfully realized for simple structures, such as folds of a single viscous layer [Hudleston and Stephansson, 1973]. There are no theoretical descriptions of large deformations for multilayer structures (with some exceptions, for example, [Rebetsky and Gushchenko, 1995]).

The use of the well-known foreland tectonotype with its fold–thrust structures for the interpretation of inner parts of folding structures (hinterland) is a characteristic feature of current investigations. Note that such an operation is open to question, because the layered medium of the latter is essentially different in its mechanical properties. It is known that the main methods used for determining the shortening value, such as the strain analysis, the method of the “excessive” length of the layer, the construction of balanced profiles, the inclusion of the Ramsay “F factor,” paleomagnetic data, etc., either relate to small structures, or do not ensure the necessary accuracy, or cannot be used in hinterland structures.

Thus, investigations of the linear folding, such as the structural reconstruction and the shortening estimation, involve serious difficulties in the formulation of the problem, which are associated with the identification of objects and the choice of the theoretical model for them on the basis of mechanics. This paper proposes a new formulation of these problems and the first solutions for them.

GENERAL APPROACH TO SOLVING THE PROBLEM

Since one of the important aspects of the solution of the problem of the linear folding formation is associated with the reconstruction (prediction) of the present-day structure into its depth and into its eroded part, it is evident that this can be done only with the use of data on the mechanisms that acted in natural structures themselves and the strain values in them. In this case, one should rely on detailed natural data rather than upon general models; i.e., in the procedures used for obtaining the result, one should move from minor structures, whose formation mechanisms and strain values are known better, toward large objects, whose present-day structures and formation mechanisms are to be revealed as a result of investigations. Of course, it is preferable to use the models of structure formation within the framework of dynamics; however, since, in the general case, the main parameters (object structure, internal and external forces, rheology, duration of loads) remain unknown, kinematic models, in which the measured geometric parameters of the structure are related in one way or another to the “amount” of the mechanism, can be used as the first step. From this point of view, geometric properties of each, even small, fold can contain sufficient information for the solution of such problems.

The choice of the object of the investigations, more exactly, the determination of its boundaries is one of the most substantial parts of the formulation of any problem. As was shown previously [Yakovlev, 2008a], the use of the generally accepted notions of structural geology, which were developed for mapping purposes, is not suitable in this case, because such objects correspond to precisely these purposes rather than to the determination of strain types and values. In this case, one needs to use the hierarchy system of linear fold structures [Yakovlev, 1997; Rebetsky et al., 2004], seven levels of which correspond to different volumes of the layered medium. In describing each object it is extremely important that one should try to provide such necessary and sufficient parameters of its geometry, which would completely describe its strain state. Such kinematic models establish mutual relations between the parameters of the object’s geometry and its strain type and value (“amount” of mechanism). Below, I list the specified seven levels: (1) intralayer deformations (distortion of the shape of grains and inclusions, subject to the strain analysis); (2) an individual fold (individual layers and pairs of layers); (3) a fold domain (a series of folds in a number of layers, large parts of the sedimentary cover); (4) a structural cell (structures from a local anticlinorium core to a local synclinorium core, the sedimentary cover as a whole); (5) a tectonic zone (traditional structure, encompasses a part of the crust or the whole crust); (6) a large folding system (for example, the megaanticlinorium of the Greater Caucasus, the level encompasses the whole lithosphere); and (7) the entire fold–thrust belt (the depth of the structure probably exceeds the thickness of the lithosphere). Structures of four levels: domains, structural cells, tectonic zones, and the folding system (partially), will be invoked

for solving the considered problem of the reconstruction (prediction) of a folding system structure (proposed for the first time in [Yakovlev, 2007]). The method will be described as an algorithm, and these structures will be briefly described as needed.

The structure of the Northwestern (NW) Caucasus was chosen as the object for testing the new approach. One of its important advantages is the fact that detailed structural profiles were previously constructed for this structure by T.V. Giorgobiani and E.A. Rogozhin [Giorgobiani and Zakharaya, 1989; Sholpo et al., 1993] as a result of specially organized field works (Fig. 1). Note that such intersections most reliably reproduce the structure. Ordinary geological intersections that are compiled from the data of geological maps with the purpose of illustrating the latter merely reflect the most general features of the structure, whereas “conceptual profiles” that, as a rule, illustrate the structure of fold systems are highly unreliable [Dotduiev, 1986; Robinson et al., 1996].

THE BOUNDARIES AND MEASURED PARAMETERS OF A FOLDED DOMAIN

Step 1: the identification of domains and measurement of all parameters. Geometric parameters of domains, i.e., parts of a structural section, which occupy a certain volume (isometric in the section) of a deformed layered medium, are the basic initial data for the proposed method (Fig. 2). In describing the deformation of domains, I will use the notion of the ellipsoid of multiplicity, whose principal axes coincide (postulate of the method) with the line perpendicular to the axial plane of the folds, the fold hinge line, and the perpendicular to the hinge line lying in the axial line. The axial plane is defined as a surface passing through the places of the largest bend of layers in the fold of a “similar” type. The plane perpendicular to the axial plane is the orientation of the axis of the maximum shortening of the multiplicity ellipsoid; in the general case, the intermediate axis is located along the hinge line. The axis of elongation lies perpendicularly to the hinge line and along the axial plane; thus, the tilt of the latter is an important deformation parameter. The components of the multiplicity ellipsoid are defined as $e = L_1/L_0$ and are related to the deformation ellipsoid as follows: $\varepsilon = \ln(L_1/L_0)$ [Rabotnov, 1979]. Such a description of the strain state of folds is sometimes met in the literature ([Nicolas, 1992, p. 120]); however, it is not widespread and is never used. The relationship between the shortening and the deformation ellipsoid itself of the domain and the ellipsoids for the volumes inside the competent and incompetent layers is described in [Yakovlev, 2002; Yakovlev and Voitenko, 2005].

Within the domain, the natural structure must unite folds of about the same shape (Fig. 2), as far as possible, with identical orientations of axial surfaces, with a relatively common tilt of the envelope plane of folds, and with relatively equal shortening values. Any significant change in one of the parameters along the profile is a reason for drawing the domain boundary. One must be careful that the domain sizes along the profile line are approximately iden-

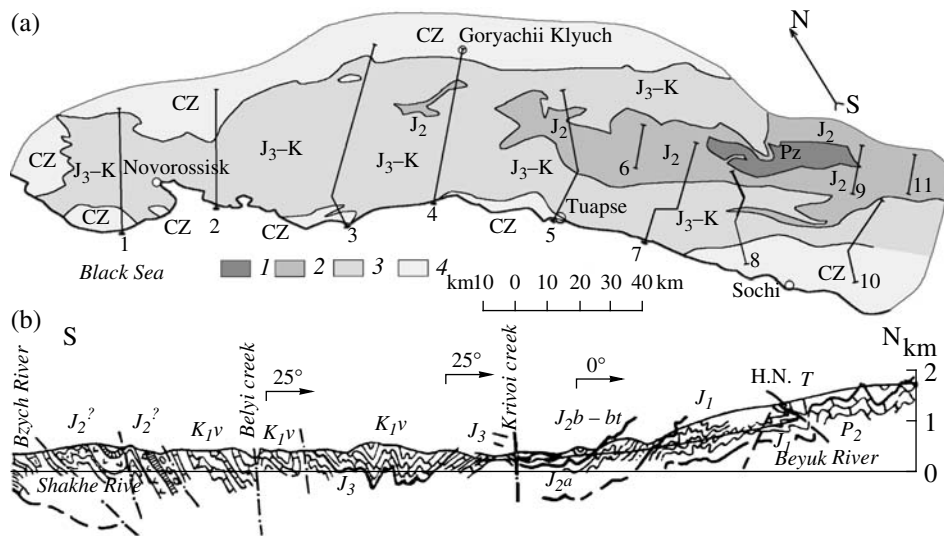


Fig. 1. (a) Schematic map of the Northwestern Caucasus and (b) example of the detailed structure for the northern half of profile 8 (data of E.A. Rogozhin in [Sholpo et al., 1993]).

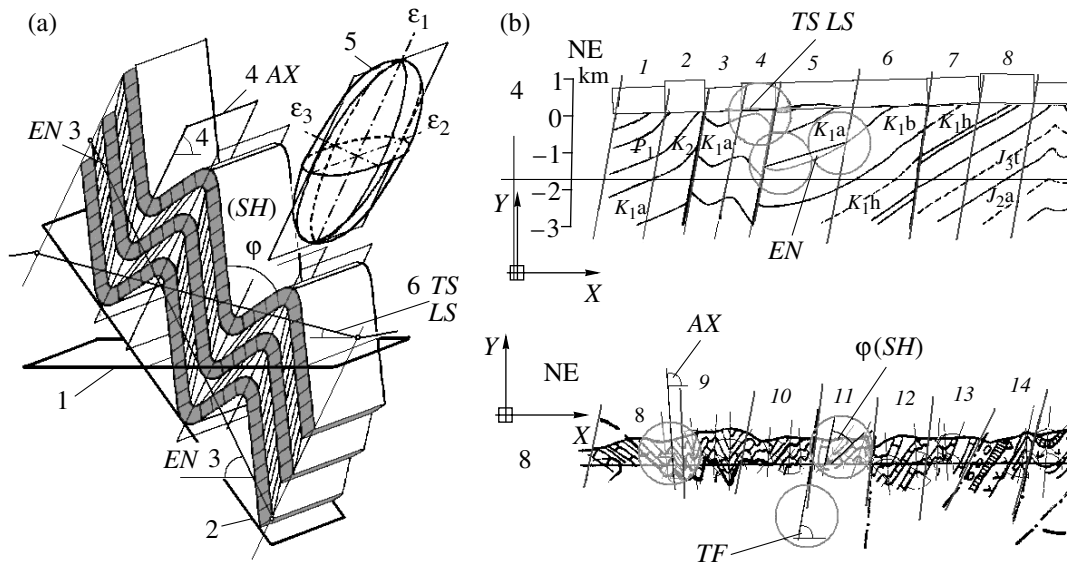


Fig. 2. Basic parameters of the domain geometry and their measurements. (a) Basic parameters (after [Yakovlev and Voitenko, 2005] with changes): (1) horizontal plane; (2) folds envelope plane (surface enveloping fold hinges); (3) line of the initial layering and its dip angle (EN); (4) axial plane of the fold and its dip angle (AX); (5) ellipsoid of multiplicity (shortening of folds in the direction of the perpendicular to the axial plane); (6) profile line segment, its length (LS) and tilt (TS); φ is the angle of convergence of fold limbs used for determination of the shortening (SH). (b) Measurements of parameters in natural structures according to the ACAD program. Profile 4 (top) (data of T.V. Giorgobiani) and profile 8 (data of E.A. Rogozhin) are shown for technical reasons in a mirror reflection; the north is on the left. Gray numerals and subvertical lines are the identified domains and their boundaries. Measurements of the parameters TS , LS , and EN in domains 4 and 5 and the parameters AX and $\varphi(SH)$ in domains 9 and 11, as well as the tilt of the fault plane TF between domains 10 and 11, are shown against the gray background.

tical. In the prefolded state, the neighboring domains must be in contact along the vertical boundaries. Since, in the general case, the initial axial surfaces are perpendicular to the horizontal layering, domain boundaries in natural struc-

tures are drawn as lines parallel to the axial surfaces. The domain is related to the space, where it is seen best, i.e., to the profile line running along the relief. For this purpose, the points of the section of the profile lines and the lines

bounding the domain are sought. Therefore, first and foremost, the following two parameters are measured in the domain: (1) the length of the rectilinear segment of the profile LS within the domain from its initial point to its end point, and (2) the dip angle of this segment TS ($\pm 45^\circ$) counted from the horizontal direction chosen for several parallel intersections (Fig. 2b, profile 4). Dip angle of several axial planes of folds (from the chosen direction, i.e., from 0° to 180° , respectively) are measured within the natural domain, and the results obtained are averaged, thus yielding the third parameter: the dip angle of the axial plane AX . Further, in the structure drawn within the domain, I choose the layer, which either intersects both its boundaries or can be easily continued to such boundaries. The straight line is drawn through the two points formed by the section of this layer and the domain boundaries, and its dip angle will be the next, fourth, measured parameter: the dip angle of the line of the initial layering EN (an analog of the folds envelope plane, $\pm 90^\circ$). Note that the special methods based on models of mechanics (or kinematics), which use parameters of the layer geometry as measured parameters [Yakovlev, 1978; 2008b], should be, in principle, used for determining the shortening of folds. However, if special field works were not carried out, the simplest method, i.e., determination of the shortening from the angle between the fold limbs ϕ , can be used (Fig. 2b, profile 8):

$$SH = \sin(\phi/2). \quad (1)$$

The experience of the use of special methods in the Caucasus makes it possible to state that in the very first approximation, such an estimate will be sufficiently accurate. For natural structures, this angle is measured in several folds, the shortenings are determined for them, and the result of their averaging will be the last, fifth, parameter characterizing the ellipsoid: the shortening SH in the direction of the perpendicular to the axial plane. In terms of mechanics, this parameter corresponds to the ellipse of multiplicity.

The presence of ruptures is an important feature. Of course, if a fold medium is disturbed by a fault with displacement, the domain boundaries must go through the point of section of the profile line and the fault. This will be the additional, sixth, parameter: the dip angle of the plane of such a fault TF , which will be needed for the balancing of the profile. This parameter is measured in accordance with the rule for measuring the dip angle of the axial plane (Fig. 2b, profile 8).

Below, I outline some tasks and assumptions. First of all, these include the postulate of the volume constancy within the domain, without which it is impossible to calculate deformations, and the postulate of the existence of a two-dimensional deformation, or a constancy of area in the plane of a structural section. Undoubtedly, there is a phenomenon such as the consolidation of sediments in the process of lithogenesis. This raises the question of whether this consolidation will affect the result. Since, precisely the thicknesses, which can be measured at present, i.e., after the completion of the lithogenesis of the rocks, are used for calculating the thickness of the sequence, this process has

no influence on the accuracy of the result. Two similar questions, on the size of the scales of the introduction and exportation of substance and the role of tectonic flow, are intensely discussed in the geological literature. Since the method proposed in this paper is numerical (measurements of parameters of natural structures and the exact procedures of their transformations are used in this method), any additional parameters can be included in the procedures only if these parameters can be measured. I am not familiar with any published results of such attempts, and the more so, any detailed data for the NW Caucasus, whose structure is analyzed here. Without questioning the existence of the phenomenon of "solution under pressure" for calcite and quartz grains, note that the dissolved substance is transferred, as a rule, for short distances of a few meters; therefore, on the scale of the domain (linear dimensions of about 0.3–2 km), the balance of the substance must not change. For the same region, the range of action of "the tectonic flow" for structures is supposedly a few kilometers, both along the strike and in the vertical direction [Marinin and Rastsvetaev, 2008]; however, no reliable data on the indicators, which would testify in favor of the real development of such processes, were presented.

Running somewhat ahead, note that the vertical position of the layering is also digitized: a stratigraphic model of the sedimentary cover is developed for each domain. In this model, each layer has its own depth of occurrence. Accordingly, the profile line, depending on the relief tilt, the tilt of the line of initial layering, and other parameters, will be displaced from one depth to another. When the profile line crosses the fault, the depth of the layer must be determined anew in the next domain.

OPERATIONS FOR RECONSTRUCTING THE PREFOLDED POSITION OF THE DOMAIN

Step 2: description of kinematic operations for reconstructing the prefolded position of the domain. The set of geometric indicators and the postulate of the constancy of the cross section ensure the unambiguity of the description of the of the ellipse multiplicity. The orientation of the folds envelope plane is also known as an element of the initial position of layering. Using three simple kinematic transformations, one can find the position of the profile line segment in the initial horizontally-layered medium for the zero final deformation (in this case, the ellipse of multiplicity is transformed to a circle).

The initial parameters will be designated as follows: AX_0 is the dip angle of the axial plane; EN_0 is the dip angle of the initial-layering line; SH_0 is the shortening of folds in the direction of the perpendicular to the axial plane; LS_0 is the profile segment length; TS_0 is the dip angle of the profile segment; and D_1 is the layer depth at the initial point of the domain (remains unchanged and is used for calculating the depth of the end point D_2).

I will follow the parameter changes during three consecutive kinematic operations: (1) the rotation of the envelope plane to its horizontal position; (2) the simple shearing

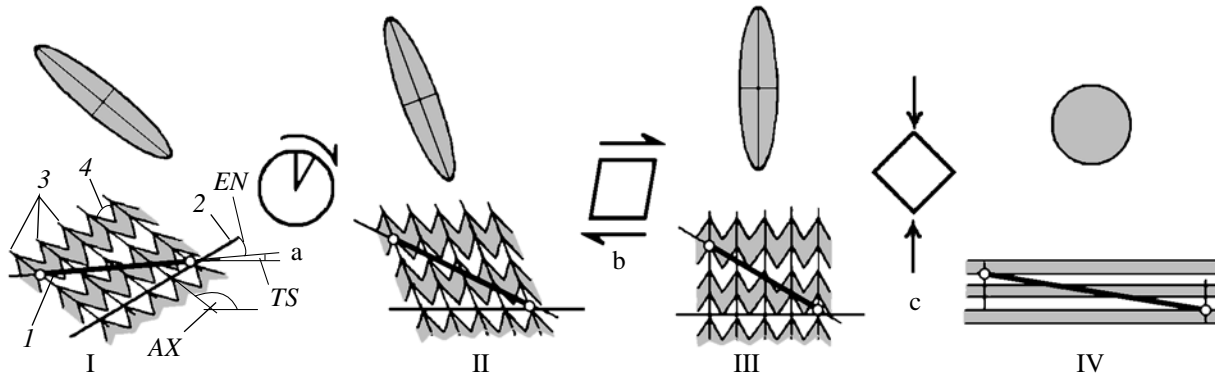


Fig. 3. Kinematic operations for reconstructing the prefolded state of the domain (after [Yakovlev, 2008c], with changes). The figure shows symbolic presentations of the fold structure of the domain from the present-day state (I) to the prefolded state (IV), deformation ellipses corresponding to the same states of the domain, and the operations: (a) rotation (from state I to state II), (b) simple horizontal shearing (from II to III), and (c) extension (pure vertical displacement from III to IV): (1) profile line segment; (2) line of the initial layering (folds envelope plane); (3) axial surfaces of folds; (4) interlimb angle of fold.

of the axial plane along the horizon to its vertical position; and (3) the maximum shortening along the horizon to reduce the multiplicity ellipse to a circle (through a pure shearing). The operation of the rotation (Fig. 3a) for the rotation angle $\Delta\alpha = -EN_0$:

$$AX_1 = AX_0 + \Delta\alpha, \quad (2)$$

$$TS_1 = TS_0 + \Delta\alpha. \quad (3)$$

The shortening of folds and the length of the profile segment remain unchanged: $SH_1 = SH_0$ and $LS_1 = LS_0$.

The operation of simple horizontal shearing (Fig. 3b) for the angle of shearing $\Delta\gamma = 90^\circ - AX_1$:

$$SH_2 = SH_1 / \sin(AX_1); \quad (4)$$

$$\tan(TS_2) = \quad (5)$$

$$\tan(AX_1) \tan(TS_1) / (\tan(AX_1) - \tan(TS_1)),$$

$$LS_2 = (LS_1 \sin(TS_1)) / \sin(TS_2). \quad (6)$$

The operation of horizontal elongation (Fig. 3c) for the extension (shortening of folds) SH_2 :

$$\tan(TS_3) = \tan(TS_2) \times SH_2^2, \quad (7)$$

$$LS_3 = LS_2 \times SH_2 \sin(TS_2) / \sin(TS_3). \quad (8)$$

After that, the profile segment will occupy the following positions in the prefolded medium:

the horizontal position

$$L_h = LS_3 \cos(TS_3), \quad (9)$$

and the vertical position

$$L_v = LS_3 \sin(TS_3). \quad (10)$$

Accordingly, the depth of the layer at the end point will be:

$$D_2 = D_1 + L_v \quad (11)$$

The chosen order of operations is not unique. Other variants may differ in the amounts of rotation, simple

shearing, and elongation, as well as in the orientations of these motions; however, regardless of the order in which these operations are performed, the result will be unchanged: for the horizontal layering and in the absence of folds, the prefolded tilt and the profile segment length will be the same as in the variant presented above.

Step 3: the reconstruction of dip angles and amplitudes of displacements on faults. If the initial point of the domain coincides with the fault, the measured dip angle TF of the fault is subjected to transformations. If $TF < 90^\circ$, the working value of the dip angle F will be equal to TF , and if $TF > 90^\circ$, then $F = TF - 180^\circ$. After that, the dip angle of the fault plane will be expressed in the same way as the dip angle of the line of the profile segment. Accordingly, all of the three kinematic operations can be repeated for the orientation of the fault plane with the use of formulas (3), (5), and (7), in which TS is replaced by F . As a result, I calculate the initial prefolded dip angle of the fault plane. The vertical displacement is specified by the depth of the layer at the end point of the preceding domain and by the depth of the layer at the initial point of the current domain, and then the horizontal displacement is determined in terms of the tangent of the tilt.

Step 4: the joining of the prefolded states of domains for the entire profile. Having the individual prefolded states of all domains and taking into account the displacements on fault planes, it is then easy to splice them together to form a specific structure, i.e., a horizontally layered medium, where profile line segments occupy a fully defined position for each domain. Accordingly, it is possible to calculate the horizontal shortening SH_{sec} of the entire profile (or its parts) as the ratio of the position of the present-day profile LF to that of the prefolded profile LP :

$$SH_{sec} = LF/LP, \quad (12)$$

where $LF = \sum LS_{0i} \cos(TS_{0i})$, and $LP = \sum L_{hi}$.

For constructing the initial structure from geometric dimensions of the domains and for the visualization of the

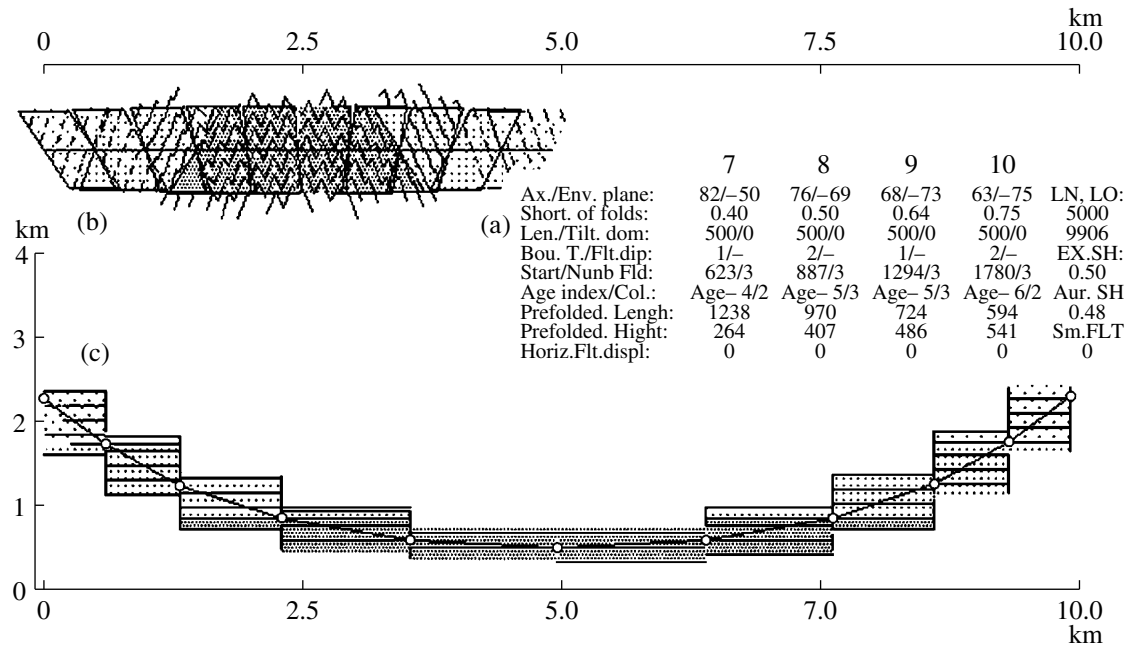


Fig. 4. Computer program of reconstructing the prefolded structure of the section operating in the DOS medium (own), which has three information fields in the display (after [Yakovlev, 2008c], with changes): (a) table of current values of measured (first six rows) and calculated (three lower rows) parameters of domains and the total result (last column); (b) model of the fold structure constructed from parameter measurements; and (c) reconstructed prefolded structure of the entire section. The error of calculations is about 1%. The figure is compiled from several display copies. Different speckles in the domains emphasize stratigraphic levels of the layered sequence; distances are arbitrary.

results of reconstruction, I use a computer program in the DOS format (Fig. 4). The general pattern of present-day and prefolded structures can be compiled in the graphics editor from the corresponding display copies. The model was formed in two stages: (1) the convective stage, which formed a large structure and (2) the homogeneous twofold shortening. The result of the reconstruction for ten domains yielded a calculation error of about 1%. Note that at the stage of calculations, one can introduce some corrections for a better correspondence of the pattern obtained for the stratigraphic model, because deviations from natural values of orientations of 3° – 5° (or up to 5% for the shortening) can be caused by various factors: from in situ measurement inaccuracies to errors during the averagings. Such refinements resemble the selection of structure variants during the standard balancing of structural intersections within the foreland.

STRUCTURAL CELL AND TECTONIC SHORTENING

Step 5: the stratigraphic model of the domain and the use of objects of the hierarchic level of a structural cell. The data collection and the formation of the stratigraphic model for each domain is one of the most important stages of reconstruction of the prefolded state, of both one structural profile and the entire structure. In order to do this, I use mainly two sources: published data and direct measurements of the thicknesses of stratigraphic units in

sections on limbs of large folds. Finally, I form a table, in which the rows located from top to bottom indicate for each domain the thickness of each stratigraphic unit (from young to ancient) and the accumulated depth (Table 1). Deposits of the Toarcian stage of the Lower Jurassic are the oldest deposits, which are assumed to be widespread in the entire analyzed volume in the NW Caucasus. The upper part of the sedimentary cover, namely, the base of the Oligocene (the base of the Maikopian series) is assumed to be zero, because, up to the first approximation, the main folding and the horizontal shortening of the structure are confined precisely to the Eocene–Oligocene boundary. The sedimentary cover's thickness attains 17 km (at its minimum of 7–9 km).

In order to determine the shortening caused by tectonic factors, one must take into account the possible influence of the disharmony associated with deviations of the field of deformations in local structures. For this purpose, I will investigate the field of deformations in a “structural cell” (the term was introduced by M.A. Goncharov [1988]). This model can be easily transformed into the model of a quasi-buckling, if an external homogeneous shortening is imposed (Fig. 5). The horizontal shortening increases the vertical dimension of the cell, and the shortening size can be selected in such a way that the length of the middle layer remains constant. I will now follow the shortening of structures in this quasi-buckling model using several segments, laid in the initial undeformed positions of two adjacent cells, as an example. The structures (segments) located in

different settings have different shortenings. It is segment (no. 3), which rests on the cell's boundaries, which has the tectonic shortening. This means that the influence of the folding disharmony can be minimized, if structural cells, approximately isometric in cross section, can be selected for determining the tectonically-caused shortening, and precisely their shortening will be measured.

For solving this problem, one must select structural cells, whose widths across the strike are approximately equal to the thickness of the entire layer (cover). Technically it is implemented as a table, where prefolded profile segments are summarized with allowance for displacements on ruptures. When the accumulated prefolded length of the section approximately coincides with the layer thickness (Table 2), one should make sure that there is no large fault or a change in the total tilt of envelope of folds; otherwise the cell boundary must be drawn at such a place. Comparing the total lengths of the profile segments in the present-day structure with the prefolded profile length, one determines the shortening value. The operation is repeated for the remaining domains the necessary number of times, until several cells are formed, depending on the total thickness of the cover and the total length of the profile.

Fault amplitudes are taken into account in the following way. If the ruptures are located inside the cell, the amplitudes of their horizontal displacements will be summarized with the total shortening. However, if a fault with a substantial displacement is located at the boundary between two cells, this displacement will be either related to one of the cells or will be divided in equal parts between the neighboring cells. Since thicknesses of sediments sharply change at the boundaries of tectonic zones, determination of the displacement amplitude is directly related to the two neighboring models of the sedimentary cover (Fig. 6). In this case, for example, young sediments in the hanging block (for a thick cover in the hinterland) can correspond to a thrust over the structure of the median massif with a reduced section rather than to a normal fault. Additionally, if the displacements have large amplitudes, there is no guarantee that the calculations based on measurements in the local structure (domain 0.3 km) will not distort the general structure (cell 7–10 km).

Step 6: construction of the map of shortenings. After the shortening values are obtained for all of the selected cells, one can start constructing the map of shortenings and verify the uniformity of the distribution of this parameter along the strike of the entire structure of the NW Caucasus. For this purpose, the northern parts of the intersections are attached to the same coordinates, because the Akhtyrsk fault located here serves as a boundary between the fold structure and the platform structure (the Kuban depression). Two variants of intersections: in the present-day coordinates and in the prefolded coordinates, are drawn in the map (Fig. 7). In accordance with the geological map and the boundaries of tectonic zones, I performed the interpolation of boundaries for all 42 structural cells.

Table 1. Calculation of the thickness of the sedimentary cover at the end of sedimentation (stage 1) for two domains of profile 8; the increase in the average thickness at shortening 0.66 (stage 2), and the depth (height) after a rise by 12257 m at a relief height of 309 m (stage 3). The thicknesses of some units and the depths of their bottoms are indicated in meters

Unit	Domain 9	Domain 10	Stage 2	Stage 3
thickness	0	0	0	
Pg ₂₋₁₊₂	0	0	0	11 948
thickness	150	150	227	
Pg _{1-il}	-150	-150	-227	11 721
thickness	150	150	227	
K _{1-al}	-4850	-4850	-7348	4600
thickness	650	650	985	
K _{1-ap}	-5500	-5500	-8333	3615
thickness	600	600	909	
J _{3-t}	-8600	-8600	-13 030	-1082
thickness	900	900	1364	
J _{3-km}	-9500	-9500	-14 394	-2446
thickness	800	800	1212	
J _{1-toar}	-15 100	-15 100	-22 879	-10 931
thickness	1000	1000	1515	
J _{1-plin}	-16 100	-16 100	-24 394	-12 446
basement	-16 100	-16 100	-24 394	-12 446

Comments on the subsequent steps of the algorithm. Since I collected the data on the thicknesses of the entire sedimentary cover (for all 42 cells), and the prefolded widths of all cells is known, it is possible to con-

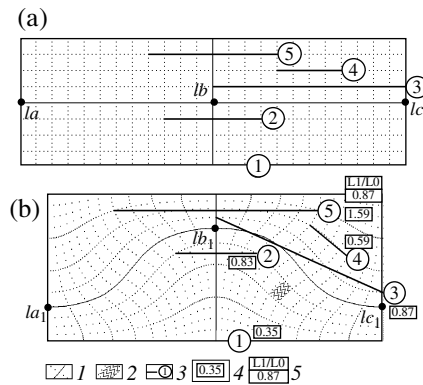


Fig. 5. Structural cell as the minimum structure, whose shortening coincides with the tectonically controlled horizontal contraction of the sedimentary cover (after [Yakovlev, 2008a], with changes): (a) two adjacent cells in the initial state and (b) the same two cells after the action of quasi-buckling: (1) initial grid and its distortion; the continuous line connecting the points *la*, *l*, and *lc* retained its length; (2) symbolic presentation of folds within a conventional domain; (3) segment and its number; (4) horizontal shortening for a segment; (5) total shortening for cells.

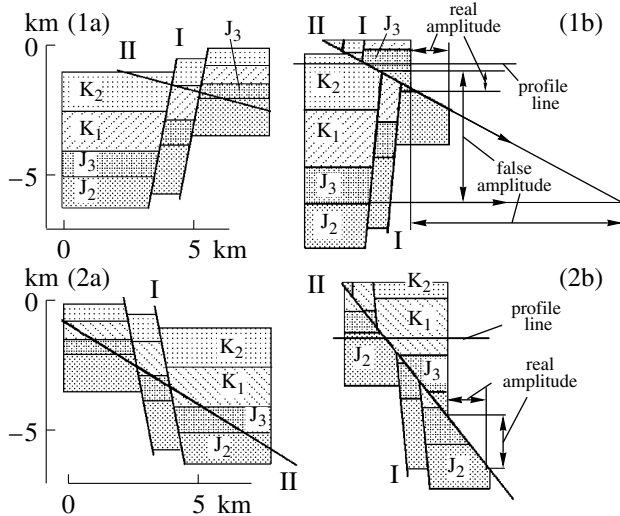


Fig. 6. Determination of the shortenings on faults at the boundaries of two facial zones with the use of tectonic structures as examples: (a) initial prefolded state; (b) post-fold state with a developed thrust; (I) growth ruptures; (II) cofold ruptures. The figure shows conventional sequences of different ages, the present-day profile line, and false and real amplitudes.

struct a model of the prefolded stage of development of the NW Caucasus (stage 1). In my opinion, at stage 1, the upper parts of the Eocene are located at the sea level. From the main angular unconformity, the age of folding was determined as the boundary between the Eocene and Oligocene (36 Ma) [Milanovskii and Khain, 1963]. It is also

known that the first conglomerates pointing to the beginning of the rise of the mountainous structure appear only in the Sarmatian deposits (14 Ma). In this connection, a model, in which the entire shortening of the space in the cells occurs due to the plunge of the column base of sediments with a new thickness (stage 2), is proposed as an extremely simplified variant. After determining the erosion extent and the corresponding amplitude of the rise of this column of sediments, it is possible to establish the present-day depths of the sedimentary cover base within 42 cells. This is the present-day postorogenic stage (stage 3).

THREE-STAGE QUASI-THREE-DIMENSIONAL MODEL OF THE NORTHWESTERN CAUCASUS STRUCTURE

Step 7: the construction of a prefolded postsedimentation model of the sedimentary cover of the NW Caucasus (stage 1). In accordance with the data on the accumulated thicknesses of the sedimentary cover that are averaged for each cell and the width of the prefolded structure within these cells, I constructed prefolded profiles for all intersections, including the Jurassic bottom/basement, Jurassic/Cretaceous, and Cretaceous/Paleogene boundaries (Fig. 8a). Then, in accordance with the map showing the prefolded boundaries of cells, I united these intersections to form a quasi-three-dimensional model. This model allows one to see the character of the distribution of the crust-downwarping amplitudes, i.e., the maximum downwarpings to 17 km in the western part of the region with the outlined central axis (the southern wall of the structure is not seen), smaller downwarpings to 10–15 km along the

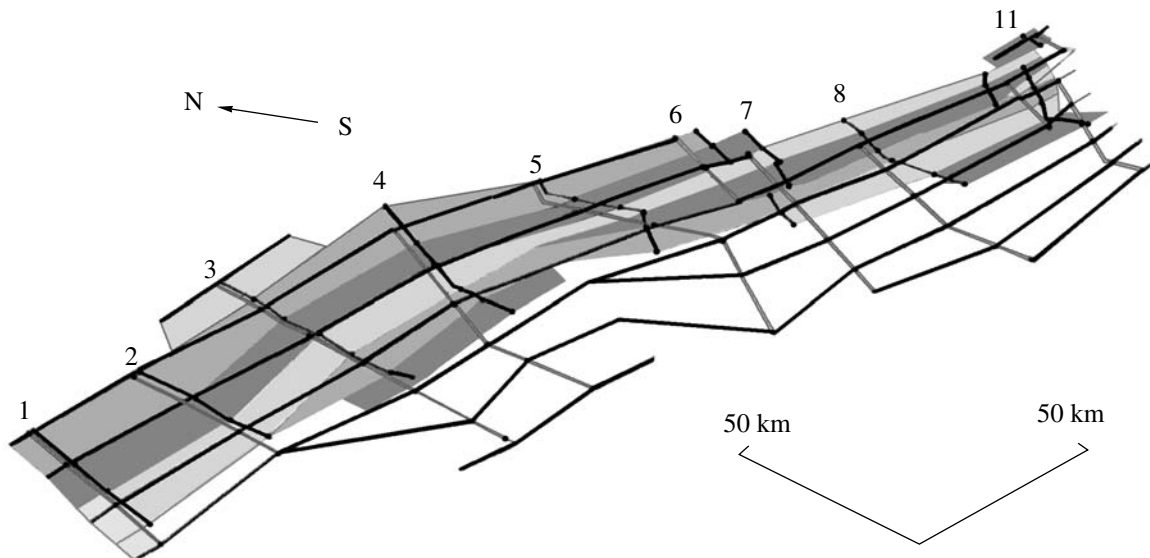


Fig. 7. Map showing the prefolded (stage 1) and present-day (stages 2 and 3) positions of the boundaries of structural cells in the axonometric projection. The black lines with numerals indicate the present-day positions of structural intersections, and the gray (longer) lines correspond to the prefolded intersections. The points on the intersections and the subparallel lines connecting them are the boundaries of cells in the prefolded and present-day coordinates. The coloring with different shades performed for the present-day coordinates of the cell boundaries emphasizes their configuration and the chosen variant of interpolation.

central axis in the eastern part, and downwarplings of 7–9 km at the edges of the structure.

Step 8: the determination of the postfolded height (depth) of the column and construction of a postfolded preorogenic model (stage 2). From the data on the initial thickness of the sedimentary cover and the shortening values for cells, I determined new postfolded thicknesses of the cover for all cells. Based on these data and the present-day coordinates of the cell boundaries, I constructed the postfolded profiles for all intersections, including the same boundaries of stratigraphic units (Fig. 8b). Further, these intersections were united within the map to form a quasi-three-dimensional model. According to the hypotheses for stage 2, the maximum (by 49 km) subsidence of the basement top took place in cell 5D with an initial thickness of 16.1 km and a shortening of 67%.

Step 9: the determination of the stratigraphic depth of the present-day section. Since, for each domain, the layer depths are determined at the initial and end points, one can determine the mean depth for the profile line segment, and the mean profile depth for the cell. In addition, I know the height of the relief of the initial point of each profile and, consequently, can easily calculate the mean heights of each domain and the entire cell. Thus, within the framework of my assumptions, I can determine the amplitude of the rise, which will bring the deposits accumulated in the given cell to the height of the present-day relief. The mean rise was about 10 km.

After all calculations for all structural cells were performed (Table 3), I calculated the present-day structure of the surface of the basement at the intersections of all stratigraphic boundaries under consideration (Fig. 8c) and constructed a quasi-three-dimensional model of the whole structure (Fig. 9). The obtained surface of the basement forms a complex but quite regular pattern. The depths of the base vary from 2–5 to 25–30 km, averaging 13 km for the structure.

DISCUSSION OF THE RESULTS

Let us discuss to what degree the data of the constructed three-dimensional model of the present-day structure of the sedimentary cover (stage 3) corresponds to the results obtained by other researchers and the geophysical data. In the recent interpretation of the complex geophysical section along the Tuapse–Khadyzhensk profile [Shempelev et al., 2001], the data on the relief of the sedimentary layer base nearly coincide with the values obtained by me for the same section (Table 3, profile 5): from north to south, this boundary decreases from 7–8 to 23–30 km. At the same time, the “conceptual” structure for the same section shows the discussed boundary as a surface of the total detachment at a depth of 5–7 km [Robinson et al., 1996]. It should be noted that the last section is very schematic; the authors who compiled it clearly did not try to take into account the

Table 2. Procedures of the selection of cells for profile 8 and the determination of shortenings. The postfolded domain lines and displacements on ruptures (columns 2 and 3) are summarized, and when they become approximately equal to the cover thickness (9 km for cell 8A and 11 km for cell 8E), the cell boundary is drawn. The total length of the present-day section (columns 5 and 6) are calculated, and the ratio of the lengths for the cell (column 7) yields the shortening

Do-main	fault amplitude	Do-main distance	Accu-mulated sum	Do-main length	Cumulative length	Shortening
1	0	1377	1377	762	762	8A
2	-147	2731	3961	1199	1961	
3	0	1538	5499	988	2949	
4	0	2859	8358	881	3830	
5	0	979	9337	695	4525	
6	0	1171	10508	1102	5627	0.54
23	0	2390	47300	1240	27498	0.77
24	0	2196	49496	1877	29375	8E
25	0	1774	51270	1613	30988	
26	0	2153	53423	1672	32660	
27	0	2183	55606	1800	34460	0.84

balance of the rock volumes of the sedimentary cover and to bring it in line with a specific natural structure.

A comparison of the proposed geodynamic models of the formation of regions with the obtained sufficiently reliable three-dimensional structure of folding zones is one of the progressive results, which can be obtained on the basis of the proposed algorithm. This comparison makes it possible to reject as impossible the models, whose geometry contradicts the balanced structure obtained on the basis of an understandable algorithm and on the basis of measurements of the natural geometry of the folds. By using the obtained geometry of the top of the basement, it was established that for the formation of a folding, large blocks of the crust must subsidence to substantial depths, which made it possible to propose a new geodynamic model of the development of the Caucasus [Yakovlev, 2008c].

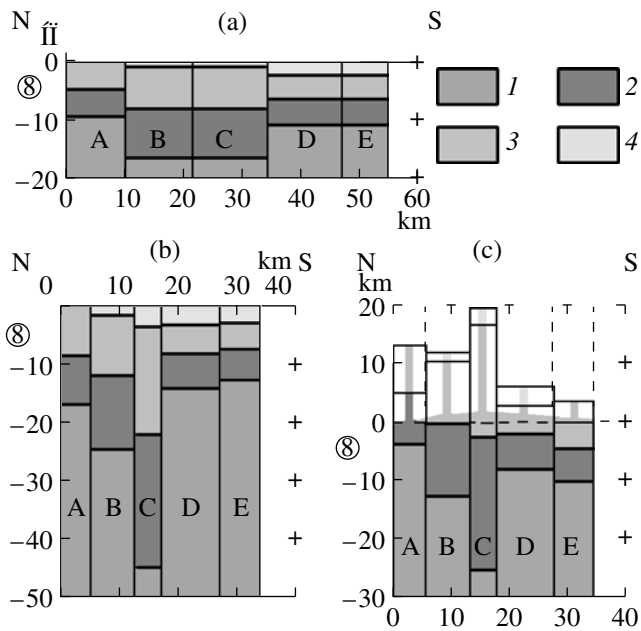


Fig. 8. Calculated structures of the surface of the basement and the main stratigraphic boundaries with the use of section 8 for five cells (A–E), as an example. The vertical and horizontal scales are the same: (a) structure for the pre-folded state (stage 1), (b) structure for the postfolded pre-orogenic state (stage 2), and (c) structure for the postorogenic present-day state (stage 3). Thin lines show the thicknesses of eroded deposits. In the sections, different shades of gray color show: (1) Paleozoic metamorphic basement; (2) Jurassic deposits; (3) Cretaceous deposits; (4) Paleocene and Eocene deposits.

It is difficult to elucidate the question concerning the accuracy of the constructions in a single paper, due to the presence of many steps in the proposed algorithm, and errors can both accumulate and be neglected. For example, if a large fault and a layering in one of the blocks are sub-parallel, the accuracy of in situ measurements of geometric elements of the structure must be very high, because small deviations have a substantial influence on the angle of the prefolded tilt of the fault plane and, consequently, on the amplitude of the displacement. The accuracy of the stratigraphic model is an important aspect: the results of calculations of the depth of the cover base, the volume of eroded rocks, as well as the calculated displacement amplitudes of the thrusts at the boundaries of tectonic zones, depend on this parameter. However, on the whole, one can assume that the data on horizon depths can differ by 10–15%, which can be caused by some small deviations in the geometric measurements of domains and their stratigraphic models, although the general character of the structure and the mean values of the structural parameters are undoubtedly retained.

The proposed approach from the standpoint of mechanics successively combines two different concepts of the description of the deformation for structures of different sizes: ellipsoid for intralayer structures, bend for folds, ellipsoid for domains, and bend for the entire sedimentary cover in structural cells. This approach makes it possible, at the level of kinematic models, to decode structures, which cannot be described as yet at the level of dynamics.

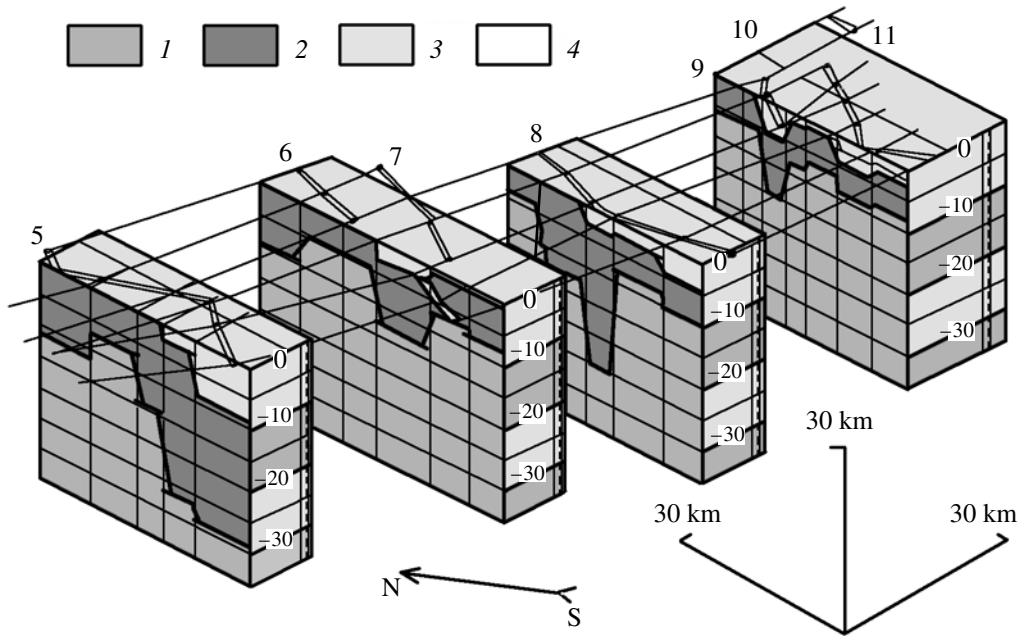


Fig. 9. Postorogenic present-day structure of the Mesozoic–Cenozoic sedimentary cover of the Northwestern Caucasus (stage 3) shown as a quasi-three-dimensional model in the axonometric projection for the eastern part of the region. The notation is the same as in Fig. 8.

Table 3. Data on the shortenings (columns 2–4), initial thicknesses of the sedimentary cover (stage 1, column 5), and basement top depths (stage 3, column 6) for 42 structural cells (indices in column 1: the number of section and the index of cell from north to south). The lengths and shortenings for individual sections are bold-faced)

1	2	3	4	5	6	1	2	3	4	5	6	1	2	3	4	5	6
	Prefolded length	Present-day length	Shortening	Bottom J	Bottom J		Prefolded length	Present-day length	Shortening	Bottom J	Bottom J		prefolded length	Present-day length	Shortening	Bottom J	BottomJ
1A	13.6	14.5	1.07	-17.0	-13.3	4D	9.7	4.7	0.48	-16.2	-20.7	8A	10.5	5.6	0.54	-9.1	-3.6
1B	18.8	11.7	0.62	-17.0	-22.7	4E	16.6	8.0	0.48	-16.3	-27.3	8B	11.4	7.5	0.66	-16.1	-12.4
1C	17.4	15.4	0.88	-17.0	-17.1		71.7	48.7	0.68			8C	12.7	4.6	0.36	-16.1	-25.1
	49.8	41.6	0.84			5A	14.4	9.7	0.67	-12.8	-11.2	8D	12.7	9.8	0.77	-10.8	-7.9
2A	13.5	14.9	1.10	-15.2	-12.4	5B	16.3	10.0	0.61	-12.8	-7.0	8E	8.3	7.0	0.84	-10.8	-10.0
2B	16.1	11.1	0.69	-16.7	-18.8	5C	15.1	5.9	0.39	-12.7	-14.2		55.6	34.5	0.62		
2C	11.2	10.0	0.89	-17.3	-15.9	5D	13.2	4.4	0.33	-16.1	-26.6	9A	6.6	3.2	0.49	-8.8	-5.6
	40.9	36.1	0.88			5E	23.3	9.3	0.40	-16.1	-29.0	9B	11.5	7.9	0.69	-8.8	-2.2
3A	13.1	10.1	0.77	-14.2	-16.7		82.4	39.4	0.48				18.1	11.1	0.61		
3B	13.7	10.7	0.78	-14.7	-12.6	6A	12.6	6.1	0.49	-12.8	-9.4	10A	10.1	3.7	0.37	-9.8	-15.2
3C	15.2	9.6	0.63	-17.1	-16.8	6B	14.4	7.1	0.49	-12.3	-5.7	10B	6.7	4.4	0.65	-10.8	-8.3
3D	15.1	9.7	0.64	-17.1	-18.2		27.0	13.2	0.49			10C	6.9	5.5	0.80	-10.8	-6.9
3E	15.7	10.8	0.69	-17.1	-19.0	7A	13.3	7.5	0.56	-8.5	-4.4	10D	8.9	7.3	0.82	-7.6	-9.1
3F	9.5	4.4	0.47	-17.1	-31.7	7B	8.7	6.3	0.73	-11.5	-4.6	10E	7.6	6.3	0.83	-7.3	-8.6
	82.3	55.3	0.67			7C	14.6	9.6	0.66	-15.1	-13.2		40.1	27.2	0.68		
4A	15.9	15.5	0.98	-13.6	-11.6	7D	12.7	7.0	0.55	-9.8	-6.9	11A	8.3	4.9	0.59	-8.8	-5.4
4B	13.7	8.7	0.63	-16.2	-8.7	7E	9.2	4.5	0.49	-9.8	-7.7						
4C	15.8	11.8	0.75	-16.2	-12.7		58.4	34.9	0.60								

CONCLUSIONS

The method of reconstructing the prefolded structure from the geometry of domains has made it possible to construct, for the first time, a model of the folding of the hinterland (the internal part of folding structures) balanced over the volume of the entire sedimentary sequence. A complete description of the deformations with the maximum possible degree of detail is used for the purpose.

The proposed approach to the problem of folding, based on the system of the hierarchy of linear folding objects, each having its own special kinematic model of formation, allows the solution of this complex problem by parts. The consecutive increase in the linear dimensions of the objects under investigation at different stages of analysis makes it possible to obtain quantitative data on large structures, which are unrelated to any interpretation on the basis of geodynamic models. The obtained structure of the surface of the sedimentary cover–metamorphic basement fully agrees with the latest data of geophysical investigations. The quasi-three-dimensional distribution of depths of this surface displays strong but quite regular changes. Since the most widely used scheme of the thrusting of

southern crustal blocks under the Greater Caucasus contradicts these results, it is evident that the more reliable data on the real structure obtained in this work, will favor the development of new geodynamic models.

ACKNOWLEDGMENTS

I am grateful to Yu.L. Rebetsky, L.A. Sim, A.V. Marinin, and A.V. Mikhailova (Laboratory of Tectonophysics IFZ RAN), who during a recent series of workshops extensively analyzed the major aspects of the method under discussion, which substantially improved the presentation of the data.

REFERENCES

1. S. I. Dotduev, "On the Nappe Structure of the Greater Caucasus," *Geotektonika*, No. 5, 94–106 (1986).
2. T. V. Giorgobiani and D. P. Zakaraya, *Fold Structure of the Northwestern Caucasus and the Mechanism of Its Formation* (Metsniereba, Tbilisi, 1989) [in Russian].
3. M. A. Goncharov, *Mechanism of Geosynclinal Folding* (Nedra, Moscow, 1988) [in Russian].

4. P. J. Hudleston and O. Stephansson, "Layer Shortening and Foldshape Development in the Buckling of Single Layers," *Tectonophys.* **17** (4), 299–321 (1973).
5. A. V. Marinin and L. M. Rastsvetaev "Structural Parageneses of the Northwestern Caucasus," in *Problems of Tectonophysics. To the 40th Anniversary of the Organization by M. V. Gzovskii of the Laboratory of Tectonophysics at the IFZ RAN* (Ed. by Yu. L. Rebetskii, Moscow, 2008), pp. 191–224 [in Russian].
6. E. E. Milanovskii and V. E. Khain, *Geological Structure of the Caucasus. Sketches on the Regional Geology of the USSR*, Issue 8 (MGU Press, Moscow, 1963) [in Russian].
7. A. Nicolas, *Fundamentals of Rock Deformation* (Mir, Moscow, 1992).
8. Yu. N. Rabotnov, *Mechanics of a Deformed Solid* (Nauka, Moscow, 1979) [in Russian].
9. J. G. Ramsay and M. I. Huber, *The Technique of Modern Structural Geology. V. 2. Fold and Fractures* (Acad. Press, London, 1987) pp. 308–700.
10. Yu. L. Rebetsky and O. I. Gushchenko, "Equations of State and Specific Features of the Evolution of Deformation Anisotropy of Layered Massifs in the Process of Folding (Mathematical Modeling)," *Fiz. Zemli*, No. 8, 13–31 (1995) [*Izvestiya, Phys. Solid Earth*, 1995].
11. Yu. L. Rebetsky, A. V. Mikhailova, D. N. Osokina, and F. L. Yakovlev, *Tectonophysics. The Earth Planet. Encyclopedic Handbook. Vol. Tectonics and Geodynamics* (Ed. by L. I. Krasnyi, O. V. Petrov, B. A. Blyuman, St. Petersburg, 2004) pp. 121–134 [in Russian].
12. A. G. Robinson, J. H. Rudat, C. J. Banks, and R. L. F. Wiles, "Petroleum Geology of the Black Sea," *Marine and Petroleum Geology* **13** (2), 195–223, 1996.
13. A. G. Shempelev, N. I. Prutskii, I. S. Fel'dman, and S. U. Kukhmazov, "A Geological–Geophysical Model along the Tuapse–Armavir Profile," in *Tectonics of the Neogaea: General and Regional Aspects 2* (Moscow, 2001), pp. 316–320 [in Russian].
14. V. N. Sholpo, E. A. Rogozhin, and M. A. Goncharov, *Folding of the Greater Caucasus* (Nauka, Moscow, 1993) [in Russian].
15. F. L. Yakovlev, "Estimation of Deformations in a Fold Region from Disharmonic Folds," *Byull. MOIPa, otd. geol.* **53** (5), 43–52 (1978).
16. F. L. Yakovlev, *Diagnostics of the Formation Mechanism of Linear Folding from Quantitative Criteria of Its Morphology (on the Example of the Greater Caucasus)* (Ed. OIFZ RAN, Moscow, 1997) [in Russian].
17. F. L. Yakovlev, *Investigations of Processes and Mechanisms of the Development of Plicated Deformations in the Earth's Crust (Review of the Existing Methodological Approaches). Tectonophysics Today*, Ed. by V. N. Strakhov, Yu. G. Leonov (Ed. OIFZ RAN, Moscow, 2002), pp. 311–332 [in Russian].
18. F. L. Yakovlev, "The First Experience of Constructing of a Three-Dimensional Model of the Structure of a Linear Fold Region Based on Quantitative Parameters of Deformation (on the Example of the Northwestern Caucasus)," in *Fundamental Problems of Geotectonics. Proc. XI Tectonic Conference, V. 2* (Ed. by Yu. V. Karyakin, Moscow, 2007), pp. 392–396 [in Russian].
19. F. L. Yakovlev, "Multirank Deformation Analysis of Linear Fold Structures," *Dokl. Ross. Akad. Nauk* **422**(3), 371–376 (2008a).
20. F. L. Yakovlev, "Quantitative Methods of Analysis of the Formation Mechanisms of Folds and Linear Fold Systems," in *Problems of Tectonophysics. To the 40th Anniversary of the Organization by M. V. Gzovskii of the Laboratory of Tectonophysics at the IFZ RAN* (Ed. by Yu. L. Rebetskii, Moscow, 2008b), pp. 149–188 [in Russian].
21. F. L. Yakovlev, "Vladimir Vladimirovich Belousov and the Problem of Folding Origin," *Geofiz. Issled.* **9** (1), 56–75 (2008c).
22. F. L. Yakovlev and V. N. Voitenko, "Application of the Deformation Tensor Conception for the Estimation of Deformations in Different-Scale Folded Structures," in *Proc. VII International Interdisciplinary Symposium and International Geoscience Programme (IGCP-476) "Regularity of Structure and Evolution of Geospheres," September 20–25, 2005* (Exc. Edit. V. F. Akulichev, Vladivostok, 2005), pp. 66–69.
23. V. Yaroshevskii, *Tectonics of Ruptures and Folds* (Nedra, Moscow, 1981) [in Russian].